Fission fragment mass distributions based on random walk at scission point in the Smoluchowski limit simulation*

Doing-Ying Huo (霍东英)[1] Zheng Wei (韦峥)[1,2,3†] Kang Wu (吴康)[1] Yi-Xuan Wang (王艺璇)[1]
Chao Han (韩超)[1] Jun Ma (马骏)[1] Jun-Run Wang (王俊润)[1,2,3] Yu Zhang (张宇)[1,2,3] Ze-En Yao (姚泽恩)[1,2,3]

[1]School of Nuclear Science and Technology, Lanzhou University, Lanzhou 730000, China
[2]Engineering Research Center for Neutron Application Technology, Ministry of Education, Lanzhou University, Lanzhou 730000, China
[3]MOE Frontiers Science Center for Rare Isotopes, Lanzhou University, Lanzhou 730000, China

Abstract: A scission point model with dynamical effects under the assumption of the Smoluchowski limit of strong coupling governs the final mass distribution that is in remarkable agreement with experimental data. This study investigates the sensitivity of mass distribution and mean total kinetic energy to various model components, including the scission point condition, dissipation tensor, and diffuseness width. The results of neutron-induced $^{235,\,238}$U, ^{237}Np, and ^{239}Pu fission are consistent with the scission point statistical model. In the high-energy region, the calculation results of the dynamical method are in better agreement with the experimental data. This conclusion justifies the validity of using the strong coupling approach for neutron-induced actinides fission.

Keywords: random walk, Smoluchowski limit, mass distribution, fission

DOI: 10.1088/1674-1137/ae2ab1 **CSTR:** 32044.14.ChinesePhysicsC.50044102

I. INTRODUCTION

The phenomenon of neutron-induced fission of uranium was discovered in 1938 [1], and since then, research on nuclear fission has been ongoing. Fission is among the most complex processes in nuclear physics, and it involves a strong interplay between the nuclear structure and dynamics [2]. In neutron-induced actinides fission, the parent nucleus is transformed into a variety of daughter pairs characterized by different charge and mass yields and kinetic energies. The fission yield is an important physical quantity with a wide range of applications in various fields, ranging from understanding of the cosmos in astrophysical explosions to reactor operations.

In recent years, many theoretical methods have been developed to calculate and reproduce the mass distribution of fission fragments. The developed statistical [3−6] and phenomenological approaches [7−9] calculate and predict the various fission observables with reasonable accuracy, providing reliable fission yields required for applications. These methods reproduce experimental data in regions of defined parameters. As a typical statistical approach, the scission point model calculates and reproduces fission yields considering the nuclear structure of the fragments without considering any dynamical effects [5−6]. The scission point model considers the relative statistical weights of individual fragments at the time of scission. Such calculations are completely static in nature. However, the model has a significant limitation in that the choice of the location of the scission point considerably affects the final results. Although it has a strong ability to explain existing measurements, it lacks in predictive power.

A number of dynamical models have been developed to overcome this limitation. For example, microscopic models [10−12] describe nuclear fission considering an effective energy density functional theory and the time-dependent Hartree-Fock method minimized in a chosen trial subspace of the full many-body Fock space while subject to external constraints on the density distribution. This approcah is computationally intensive and time-consuming. The Langevin model [13–14] has been developed and applied to render the dynamics macroscopic for studying nuclear fission and fusion reactions, which requires the associated collective inertial-mass tensor as well as the dissipation tensor describing the coupling of the collective variables to the remaining system. The nuclear shape evolution is strongly dissipative, and therefore, significant simplification can be obtained by considering the strongly damped limit [15–16]. Randrup and Möller

Received 11 November 2025; Accepted 9 December 2025; Accepted manuscript online 10 December 2025

* This work was supported by the NSFC-Nuclear Technology Innovation Joint Fund 393 (U2167203), the National Natural Science Foundation of China (1254710130, 12527806), the Fundamental Research Funds for the Central Universities (lzujbky-2025-jdzx11, lzujbky-2023-stlt01), and the Major Science and 396 Technology Projects of Gansu Province (22ZD6GB020)

† E-mail: weizheng@lzu.edu.cn

[15–16] calculated the mass distributions of fission fragments for a large number of nuclides in the Somluchowski limit of strong coupling [17]. In this physical picture, the evolution of the nuclear shape is similar to Brownian motion. Thus, once the potential energy of fission shapes is known, the required calculations are relatively simple and amount to a random walk over the corresponding potential surface [15].

In this paper, we demonstrate the shape evolution process near the scission point with the Smoluchowski equation to govern the final mass distribution. This approach overcomes the limitation of the scission point model, namely, the static nature of the calculations. The dynamical method for calculating fission-fragment mass distributions exploits the Smoluchowski limit of strong coupling between the nuclear surface motion and the internal degrees of freedom [18], which helps ensure the calculation accuracy and is suitable for large-scale computations. The method is equivalent to a random walk on the corresponding potential energy surface as a function of deformation and the internuclear distance between fragments. This method offers a very quick and easy means to obtain practically useful fission-fragment mass distributions.

The remainder of this article is organized as follows: Sec. II provides a brief description of our proposed model. The results of the mass distribution and average total kinetic energy (TKE) distribution of fission fragments are given in Sec. III. Finally, in Sec. IV, we will provide a summary of this study.

II. METHODS

Describing the shape of the fissioning system is necessary to obtain a basis for the potential energy surface. The fragments nucleus is in a state of significant deformation when reaching the scission point. In the vicinity of the scission point, it is assumed that the neck is thin. The shape can be viewed as a system of two deformed fragments separated by distance d. The impact of the neck on the potential energy is no longer considered. The axial-symmetric nucleus can be expressed in spherical coordinates by describing the shapes of two fragments using a spherical harmonic function expansion

$$R_i(\beta,\theta) = c(\beta_{\lambda i})R_{0i}[1+\sum_{\lambda=2,3}\beta_{\lambda i}P_2(\cos\theta)]. \tag{1}$$

$R_{0i} = 1.16A_i^{1/3}$ is the radius of the spherical nucleus, where ($i = L, H$) represent the light and heavy fragments, respectively. Further, c($\beta_{\lambda i}$) represents an essential parameter on the premise of the volume conservation when the deformation parameter $\beta_{\lambda i}$ is determined, where ($\lambda = 2, 3$) denote the quadrupole and octupole deformations, respectively. In recent work [6], the authors demonstrated that the elongated deformed compound nucleus exhibits strong octupole deformation before scission. $P_2(\cos\theta)$ is the Legendre polynomial.

This paper simulates dynamical evolution using the Langevin equation for the strongly damped fission process. In this limit, the Langevin equation is reduced to the Smoluchowski equation. The shape evolution is damped and diffusive, with the driving force from the potential $F^{\rm pot}$ and dissipative force $F^{\rm diss}$ reaching equilibrium in the Smoluchowski limit of strong coupling [15–16]

$$F^{\rm pot}(x) + F^{\rm diss}(x,\dot{x}) = 0. \tag{2}$$

where x represents the dimensionless fission deformation coordinate defined above. This coordinate is specified by d/R_0, $\beta_{\lambda i}$, and η, where R_0 represents the radius of the spherical nucleus. The potential energy U provides the driving force $F^{\rm pot}(x)$, which has the components $F^{\rm pot} = -\dfrac{\partial U(x)}{\partial x}$. The potential energy is calculated by the scission point model [6]. The dissipation tensor γ governs the associated friction force $F^{\rm fric} = -\gamma\cdot\dot{x}$, which is the average value of the dissipative force $F^{\rm diss}$. As is common, the remaining interaction is stochastic and the associated force is denoted by $F^{\rm ran}$(t). This force vanishes on the average by definition, $\langle F^{\rm ran}(t)\rangle = 0$, and its time dependence is Markovian, so $\left\langle F_i^{\rm ran}(t)F_j^{\rm ran}(t')\right\rangle = 2T\gamma_{ij}\delta(t-t')$. This allows Gaussian random numbers to be used to model normalized random forces. This condition immediately yields the instantaneous velocity

$$\dot{x}(t) \doteq \mu\cdot(F^{pot}(t) + F^{ran}(t)) \tag{3}$$

Then, the net displacement accumulated in the course of a brief time interval Δt is

$$\delta x = \int_0^{\Delta t}\dot{x}(t){\rm d}t = \mu\cdot[(F^{\rm pot}\Delta t) + \int_0^{\Delta t}F^{\rm ran}(t){\rm d}t] \tag{4}$$

Subsequently, we can obtain the total increment accumulated in a very short period of time as

$$\Delta x_i = \mu_i F_i^{\rm pot}\Delta t + \sqrt{2T\mu_i\Delta t}\xi_i \tag{5}$$

where the mobility tensor μ is the inverse of the dissipation tensor γ. In addition, the dissipation tensor $\gamma = M\beta$. β represents the reduced friction parameter, which is the only parameter of this model. M represents the inertia parameter, which drops out of the strongly damped equation and can be expressed as an approximate mass. Strongly damped motion is characterized by the relative unimportance of inertial forces, which makes knowledge about the inertia-mass tensor for the shape

motion less crucial. ξ_i is a time-dependent stochastic variable with a Gaussian distribution, which enables a Gaussian random number to model the normalized random force.

The shape parameter undergoes a generalized Brownian motion in simulating the Smoiuchowski equation. The evolution of the Brownian shape requires sampling the potential energy surface using the Metropolis process, a Markov chain Monte Carlo method that evolves gradually to the target distribution by randomly selecting a new state and deciding whether or not to accept this new state based on a certain acceptance criterion.

We need to know the probability of taking a step forward or backward in a short time interval Δt, $P_{\pm}^{(i)} = v_{\pm}^{(i)}\Delta t$, where $v_{+}^{(i)} = P(x_i,t) \to P(x_i+\Delta t,t)$ and $v_{-}^{(i)} = P(x_i,t) \to P(x_i-\Delta t,t)$.

In the Fokker-Planck equation,

$$\frac{\partial}{\partial t}P(x_i,t) = \left[-\sum\nolimits_i \frac{\partial}{\partial x_i}V_i + \sum\nolimits_{i,j}\frac{\partial}{\partial x_i}\frac{\partial}{\partial x_j}D_{i,j}\right]P(x_i,t) \quad (6)$$

where $V_i = \mu_i F_i$ represents the drift coefficient, $D_i = \frac{1}{2}\times 2T\mu_i$ represents the diffusion coefficient and is equal to half the variance growth rate. In this work, the direction of each shape parameter is considered to be the eigendirection of diffusion, and then, the diffusion tensor itself is diagonalized $D_{ij} = D_{ij}\Delta_{ij}$. When $\Delta t \to 0$, we get $\frac{\langle \Delta x_i\rangle}{\Delta t} = V_i$ and $\frac{\langle (\Delta x_i)^2\rangle}{\Delta t} = 2D_i$. The formula Δx_i satisfies the following probability distribution:

$$\Delta x_i = \begin{cases} \Delta_i, P_{+}^{(i)} \\ -\Delta_i, P_{-}^{(i)} \end{cases} \quad (7)$$

These relationships can be readily solved for the rates

$$\begin{cases} (v_{+}^{(i)} - v_{-}^{(i)})\Delta_i = \mu_i F_i \\ \frac{1}{2}(v_{+}^{(i)} - v_{-}^{(i)})\Delta_i^2 = T\mu_i \end{cases} \quad (8)$$

It then follows that

$$\frac{P_{+}^{(i)}}{P_{-}^{(i)}} = \frac{T-\frac{1}{2}\Delta U_i}{T+\frac{1}{2}\Delta U_i} = \frac{1-\frac{1}{2}\frac{\Delta U_i}{T}}{1+\frac{1}{2}\frac{\Delta U_i}{T}} \approx \left(1-\frac{1}{2}\frac{\Delta U_i}{T}\right)\left(1-\frac{1}{2}\frac{\Delta U_i}{T}\right) \approx \left(1-\frac{\Delta U_i}{T}\right) \approx \mathrm{e}^{\Delta U_i/T} \quad (9)$$

According to this equation, we know that the probability of moving from the current shape to a randomly chosen shape is $\mathrm{e}^{\Delta U/T}$.

The fission-fragment mass distribution is typically calculated as follows. From the starting point, the wandering direction of the fissioning system on the potential energy surface is sampled randomly, and the Metropolis random wandering method is employed to determine if this step of wandering is accepted or not. If it is accepted, the composite nucleus is moved to a new position on the potential energy surface; otherwise, it stays in place and waits for the next wandering trial until the scission point condition is satisfied. In the Metropolis procedure, the accepted probability is $P = \mathrm{e}^{-\Delta U/T}$. Suppose that at x_n, if $\mathrm{e}^{-U(x')/T}/\mathrm{e}^{-U(x_n)/T} \geqslant 1$, then accept this trial step $x_{n+1} = x'$. If $\mathrm{e}^{-U(x')/T}/\mathrm{e}^{-U(x_n)/T} < 1$, then generate a random number ξ in the interval [0,1]. If $\mathrm{e}^{-U(x')/T}/\mathrm{e}^{-U(x_n)/T} > \xi$, then $x_{n+1} = x'$; otherwise, reject this trial step $x_{n+1} = x_n$.

III. CALCULATION RESULTS

The description of the shape of the nucleus requires a set of 7 independent parameters $\{Z_L, A_L, Z_{CN}-Z_L, A_{CN}-A_L, \beta_{2L}, \beta_{3L}, \beta_{2H}, \beta_{3H}, d\}$. However, using these parameters to calculate the dynamical evolution generates a substantial computational workload, which poses a considerable challenge for practical calculations.

To overcome this challenge, it is necessary to simplify the model employed in this paper. To this end, the mass number parameter of the light and heavy fragments are replaced by the parameter of mass asymmetry $\eta = (A_H - A_L)/(A_L + A_H)$. The fission system naturally gravitate toward the state that exhibits the lowest energy, and the fragments also exhibit a tendency to form a charge configuration that serves to minimize the potential energy. By employing this method, it is possible to ascertain a unique charge number for each individual fragment. The previous results [6] demonstrate that the quadrupole deformation parameters of the light and heavy fragments vary within the range of 0 to 0.5, while the octupole deformation of the fragments fluctuates around specific values under the effect of the interaction potential. Figure 1 shows the most probable octupole deformations of light and heavy fragments as a function of mass number. The octupole deformations of light fragments remain around 0.4, and the heavy fragments remain around 0.2–0.25. The octupole deformations come from the interaction potential between the two fragments, and therefore, it is reasonable to set the octupole deformation parameters of the light $\beta_{3L} = 0.4$ and heavy fragments $\beta_{3H} = 0.25$ as fixed values, effectively reducing the number of model parameters and lowering the complexity.

The shape of the nucleus is described by a set of shape parameters $\{d/R_0, \beta_{2L}, \beta_{2H}, \eta\}$, which include four free parameters: the distance of the fragments, quadrupole deformation for light fragment, quadrupole deformation for heavy fragment, and mass asymmetry. These are dimensionless parameters, which provide great conveni-

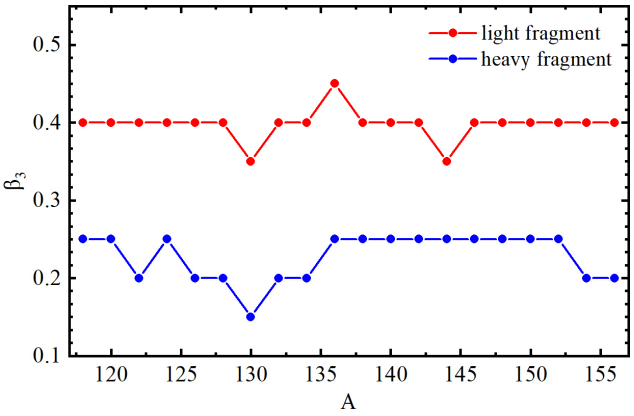

Fig. 1. (color online) Octupole deformations of scission configurations as a function of mass number for neutron-induced fission of ^{235}U.

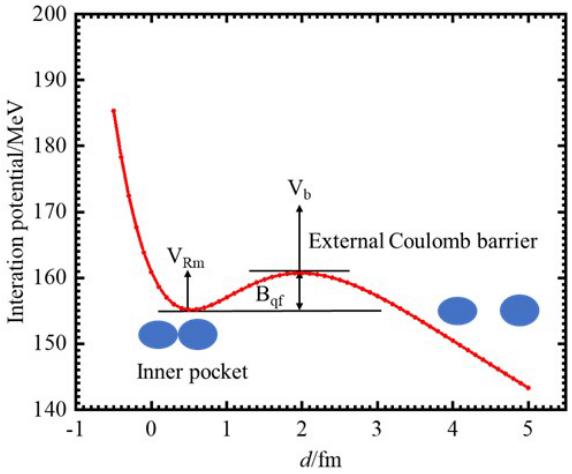

Fig. 2. (color online) Interaction potential energy of ^{96}Sr and ^{140}Xe in the reaction of n + ^{235}U.

ence for the processing of the dynamics program. A random walk on a discrete lattice based on a prepared mesh is performed to save computation time. These mesh values for d/R_0, $\beta_{\lambda i}$, and η are

$$\begin{aligned} &d/(R_0) = 0(0.014)0.35 \\ &\beta_{2L}(\beta_{2H}) = 0(0.05)0.5 \\ &\eta = -0.336(0.016)0.336. \end{aligned} \tag{10}$$

The numbers in parentheses are the mesh steps for each variable.

A. Influence of the scission point condition on the fragment mass distribution and TKE distribution

Figure 2 shows the interaction potential energy of ^{96}Sr and ^{140}Xe in the reaction of n + ^{235}U, including both the Coulomb potential barrier V_b and quasi-fission barrier B_{qf}. The evolution of the double nuclear system is a complex process involving multiple stages and critical junctures. The external saddle point V_b is indicative of a critical phase in the fission process, wherein the fissioning system has attained a local energy maximum but is yet to undergo complete division. Within this point, the fissioning nucleus is confined within a relatively stable potential well. The well originates from the interaction between the nuclear force and Coulombic force within the nucleus, establishing a temporarily stable environment. Further, the nucleus undergoes continuous oscillation, engaging in nucleon transfer and energy exchange. As oscillations persist, the double nuclear system crosses the external saddle point to reach the scission point. The transition marks the fissioning nucleus moving from a brief stable state to a complete fission state, releasing substantial energy and neutrons. The determination of the scission point is a crucial issue because it directly affects the prediction results of the kinetic energy distribution and mass distribution of fission fragments.

In this section, we investigate the effect of the scission point condition on the fragment mass and average total kinetic energy (TKE) distributions by considering the case of 14MeV n + ^{235}U fission as an example. In this paper, the scission point is defined in terms of the shape parameter d representing the distance between two fragments. As illustrated in Fig. 3, we calculated the mass distribution for distances of 2.1, 2.3, and 2.5 fm to determine the most appropriate the scission point condition. The results are not sensitive to the choice of scission point condition. In addition, the mass asymmetry remains relatively constant, which indicates that the mass numbers of light and heavy fragments are determined before reaching the scission point. Thus, the mass distribution is formed at an earlier stage rather than being determined only after the scission point. This is in line with the conclusion obtained using a microscopic approach [19].

The average total kinetic energy distribution of fission fragments is calculated, which is another important observation related to nuclear fission. It has been assumed that all interaction energy at the scission point is converted into the kinetic energy of fission fragments. The TKE is calculated by averaging the deformations of fission fragments. The total kinetic energy is the sum of the Coulomb potential V_C [20] and nuclear potential V_N [21], which is expressed as $\mathrm{TKE}(A_i,Z_i,\beta_i) = V_C(A_i,Z_i,\beta_i) + V_N(A_i,Z_i,\beta_i)$. The results are presented in Fig. 4. When the value of d is set to 2.3 fm, the TKE is in close agreement with the experimental data [22]; however, it is significantly higher near symmetric fission. This phenomenon can be attributed to the process of symmetric fission, which can stretch the nucleus over a greater distance.

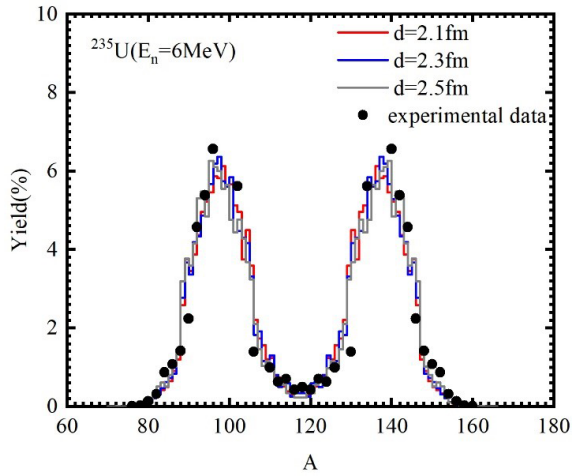

Fig. 3. (color online) Mass distributions of neutron-induced ^{235}U fission for different values of distance parameter d between two fragments.

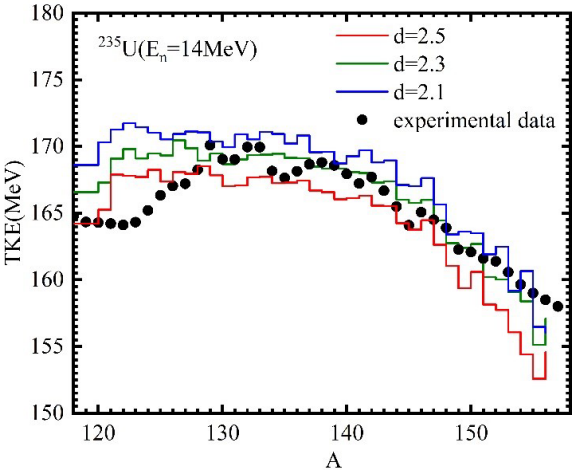

Fig. 4. (color online) Average total kinetic energy distributions of fragments of neutron-induced ^{235}U fission for different values of distance parameter d between two fragments and comparison with experimental data [22].

B. Influence of the dissipation tensor on the fragment mass distribution

The dissipation tensor is described as $\gamma = M\beta$, and β represents the reduced friction parameter, which is the only parameter of this model. Two classic deformation models have been employed in the study of nuclear fission dynamics: the standard parameter set friction (SPS-friction) model and the one-body dissipation (OBD) friction model. These models are widely utilized as representations of dissipative mechanisms in this field.

In this condition, we assumed that the dissipation tensor is isotropic in the employed lattice variables. The SPS-friction model is a simplified approach that assumes different friction coefficients during the stage of compound nucleus and subsequent elongation of the compound nucleus into fragments. In the initial fission stage, the friction parameter β remains constant until the distance between the centers of fragments reaches a certain value $r_{12} = r_{12}^{\rm neck} = 1.2R_0$. Subsequent to the formation of the neck, the friction parameter experiences a linear increase in nature with respect to the deformation until it attains the scission point. The variation in the friction parameter can be described by [23]

$$\beta_{SPS} = \begin{cases} \beta_0 & r_{12} < r_{12}^{\rm neck} \\ \beta_0 + \dfrac{(\beta_{sc} - \beta_0)}{r_{12}^{sc} - r_{12}^{\rm neck}}(r_{12}^{sc} - r_{12}^{\rm neck}) & r_{12}^{\rm neck} < r_{12} < r_{12}^{sc} \end{cases} \tag{11}$$

where $\beta_0 = 2zs^{-1}$ represents the friction parameter in compact shape, $\beta_{sc} = 30zs^{-1}$ represents the friction coefficient at the scission point, and r_{12} represents the distance between the centers of the fragments.

The factor $\beta_{\rm OBD}$ of the OBD friction model is used in an analytical fit formula developed in Ref. [23].

$$\beta_{\rm OBD} = \begin{cases} \dfrac{15}{{r_{12}}^{0.43}} + 1 - 10.5{r_{12}}^{0.9} + {r_{12}}^2 & r_{12} > 0.76R_0 \\ 32 - 32.21r_{12} & r_{12} < 0.76R_0 \end{cases} \tag{12}$$

This paper adopted the SPS-friction and OBD friction models to conduct research on the mass distribution for investigating the effect of the dissipation tensor on mass distribution. The results are presented in Fig. 5. As indicated in this figure, mass distributions calculated by the two methods are almost exactly the same, and they match the experimental data very well. The fundamental reason for this phenomenon lies in the evolution of the dynamical path being determined by the potential energy surface. Therefore, under the condition of strongly damped, irrespective of the alterations to the friction model, the fission path configuration does not undergo substantial modifications. Thus, this work proved that fragments mass distribution is not sensitive to the dissipation tensor structure (isotropy) for actinides fission, which is consistent with the conclusion obtained by Rundrup [16] using the random walk method on a five-dimensional potential surface.

C. Influence of the diffuseness width parameter on the fragment mass distribution

Nuclear densities are considered in the two-parameter Woods–Saxon form with the diffuseness width parameter $a = 0.50 - 0.58$ fm depending on the charge number of the nucleus. The diffuseness width exerts a direct effect on the nuclear density distribution function of fission fragments, consequently affecting the interaction potential energy and height of the quasi-fission barrier. The height of the barrier B_{qf} is a pivotal parameter in determ-

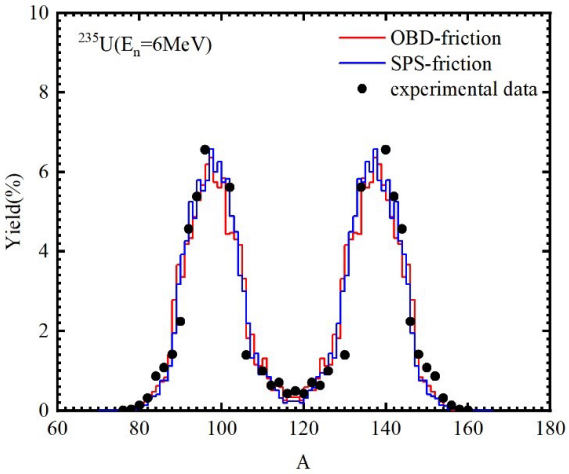

Fig. 5. (color online) Mass distributions of neutron-induced ^{235}U fission for different methods of the friction model.

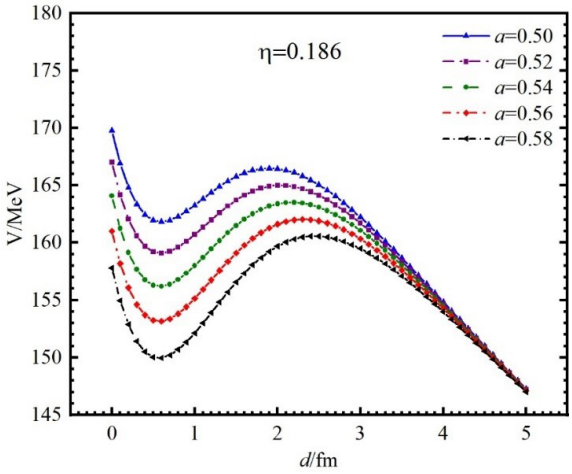

Fig. 6. (color online) Interaction potential energy of asymmetric fission.

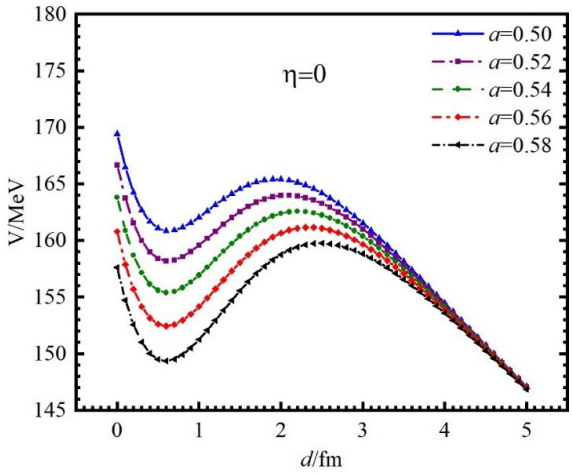

Fig. 7. (color online) Interaction potential energy of symmetric fission.

ining the capacity to surmount the fission barrier and undergo fission during the process. Consequently, the selection of the diffuseness width parameter is of paramount importance in the dynamics method.

A larger diffuseness width is indicative of a more extended distribution of nuclear densities and a "soft" nuclear surface. Consequently, the Coulomb and nuclear potentials between the double nuclear system are reduced. However, the height of the quasi-fission barrier increases gradually with an increase in diffuseness width. Figures 6−7 show that the interaction potential energy is calculated under the conditions of asymmetric fission (mass asymmetry of 0.186) and complete symmetry fission (mass asymmetry of 0). The results confirm that an augmentation in diffuseness width results in a decline in the overall interaction potential energy, which is accompanied by a gradual escalation in the height of the quasi-fission barrier B_{qf}. This phenomenon confirms that, although a larger diffuseness width renders the nuclear surface more "softer" and reduces the interaction potential below the barrier, the overall shape of the barrier becomes steeper.

To investigate the effect of diffuseness width on mass distribution, this paper compared changes in the height of the quasi-fission barrier in symmetric fission and asymmetric fission systems. The results are displayed in Fig. 8. It is evident that, as the diffuseness width increases, the quasi-fission barrier of the asymmetric fission system increases more significantly, whereas the increase in the barrier height of the symmetric fission system is smaller. This phenomenon suggests that an increase in the diffuseness width enhances the probability of symmetric fission.

The mass distribution for different diffuseness width parameters is calculated, and the results are shown in Fig. 9. The effect of distribution width on mass distribution is reflected in the peak-to-valley ratio, while the position of the distribution peak remains constant. This finding suggests that the distribution width does not significantly alter the primary mass configuration of the fission products. However, it does affect the probability distribution of the symmetric and asymmetric fission channels during the fission process.

D. The mass distribution of the fission fragments for different systems

To verify the model description, the fission fragment mass distributions in neutron-induced ^{235,238}U, ^{237}Np, and ^{239}Pu fission were calculated and compared with the scission point statistical model [6] shown in Fig. 10. The calculated results are consistent with the scission point model (without dynamics effect), especially the peak position. We know that the statistical model can adjust parameters for better results. The statistical model that does not consider the dynamics effect can control the inability of certain fragment configurations to reach the scission point by setting a minimum quasi-fission barrier B_{qf}. The in-

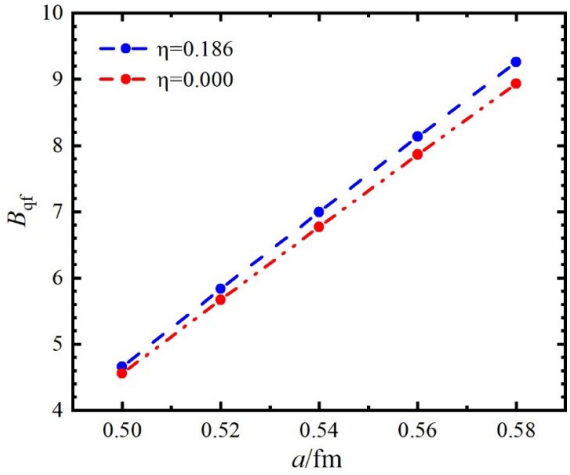

Fig. 8. (color online) Relationship between the quasi-fission barrier and the variation of the diffuseness width.

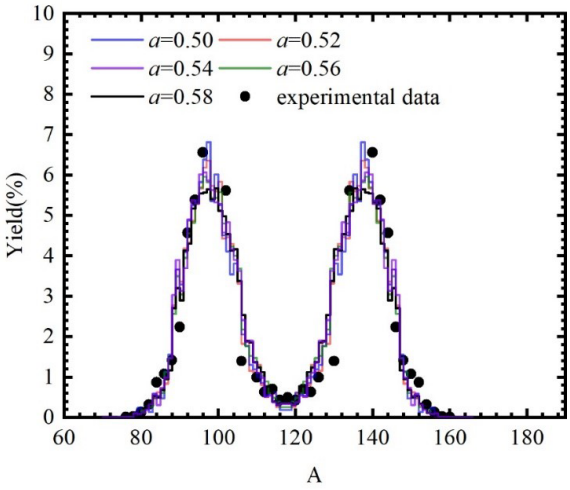

Fig. 9. (color online) Mass distribution for different diffuseness width parameters.

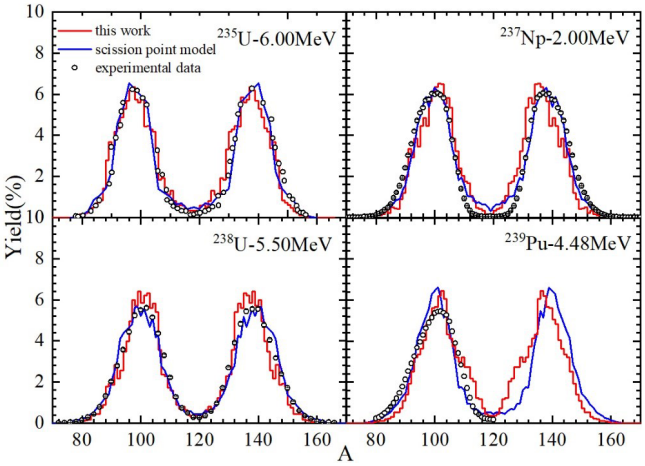

Fig. 10. (color online) Fission fragment mass distributions in neutron-induced ^{235,238}U, ^{237}Np and ^{239}Pu fission and comparison with the experimental data [24−27].

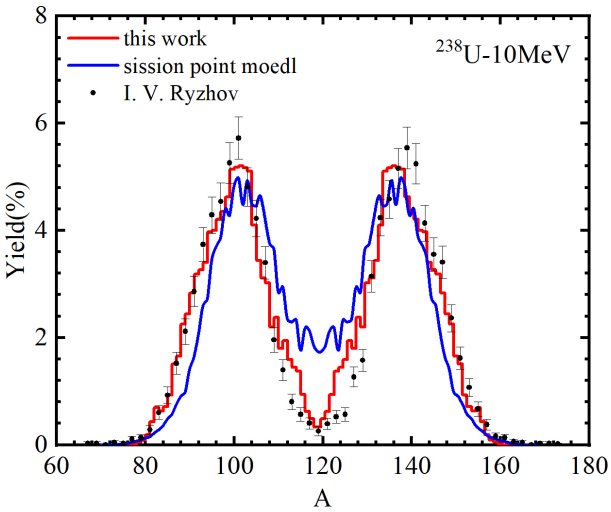

Fig. 11. (color online) Fission fragment mass distributions in neutron-induced ^{238}U fission and comparison with experimental data [28].

creased value of parameter B_{qf} can discard combinations of fragments with small asymmetry, which results in a narrow mass distribution. In contrast, the dynamics approach closely resembles the actual physical process and does not require any parameter adjustment.

Furthermore, the scission point model considers all possible light-heavy fragments and their octupole deformation parameters during its construction. A potential energy surface is constructed within the range of 9 degrees of freedom. Owing to the limitations of computing power, the model has to sacrifice some degrees of freedom when calculating the potential energy surface in this paper, which also has an effect on the results.

The mass distributions in 10 and 16.5 MeV neutron-induced ^{238}U fission were calculated and compared with the scission point statistical model. The results are shown in Figs. 11−12. The results of the dynamics approach are more in line with the experimental data. This is because the static potential energy surface can only take the extreme points of the potential energy surface in the scission point model, which is equivalent to assuming that the system is always at the bottom. The shell effect weakens as the excitation energy increases, and the potential energy surface becomes flat. The symmetric distribution result calculated by the scission point model increases suddenly. This outcome cannot be altered no matter how the value of the minimum quasi-fission barrier B_{qf} is adjusted. However, the dynamics approach adopts the Smoluchowski equation and introduce random forces, which can incorporate the deformation in real time. This enables the shape of the fission fragments to randomly oscillate multiple times. Therefore, the probability of symmetrical fission changes slowly with the variation in energy rather than suddenly jumping.

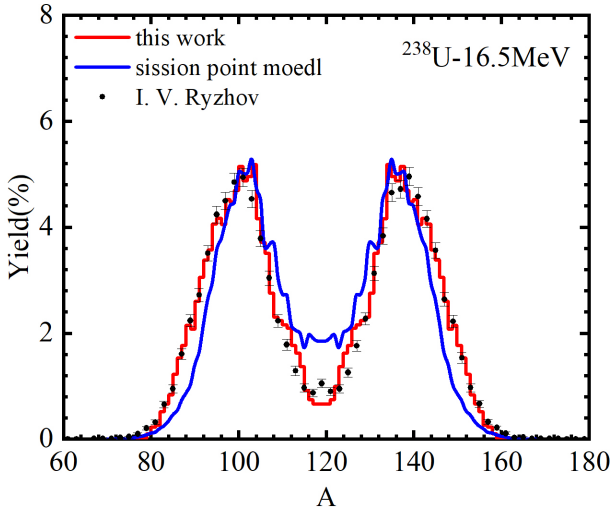

Fig. 12. (color online) Fission fragment mass distributions in neutron-induced ^{238}U fission and comparison with experimental data [28].

IV. CONCLUSION

In this paper, we consider dynamical effects based on the statistical scission point model to overcome the static nature of the calculations in the scission point model. The calculations of the type discussed here consider the idealized limit of strongly damped motion (Smoluchowski limit of strong coupling), where inertia plays no role. In this physical picture, the evolution of the nuclear shape is the same as that of Brownian motion. If the evolution of the shape in the fission process can be characterized remains an open question. However, the method provides a quantitatively useful and simple calculational tool for obtaining fission mass yields.

We investigate the effect of the scission point condition on the fragment mass and TKE distributions to determine the most appropriate choice of scission point. In addition, we studied the sensitivity of the obtained mass distribution to various model components, including the dissipation tensor and diffuseness width. Based on this, the mass distributions of neutron-induced $^{235,\,238}$U, ^{237}Np, and ^{239}Pu fission was calculated. These calculated results are consistent with the scission point model (without dynamics effects). In the high-energy region, the calculation results of the dynamical method are in better agreement with the experimental data. This confirms that this simple and somewhat arbitrary treatment (strong coupling assumption) can produce good results. This approach can be extended to obtain approximate fission yields for a large region of the nuclear chart.

This work is based on the theoretical framework of the Smoluchowski equation, and it dynamically evolves the mass distribution on the potential energy surface. However, no consideration is given to the pairing effects, and it can only handle single fission events. In addition, the shape space is limited to four dimensions. Future plans include expanding to the Th-Pu-Cm nuclide chain in batches to test the universality of the model and gradually introducing pairing effects and multi-chance fission to make this model a long-term and sustainable platform for nuclear data evaluation.

References

[1] O. Hahn and F. Straßmann, Naturwissenschaften **27**, 11 (1939)
[2] J. F. Lemaitre, S. Goriely, S. Hilaire *et al.*, Phys. Rev. C **99**, 034612 (2019)
[3] H. Pasca, A. V. Andreev, G. G. Adamian *et al.*, Phys. Rev. C **97**, 034621 (2018)
[4] H. Pasca, A. V. Andreev, G. G. Adamian *et al.*, Phys. Lett. B **760**, 800 (2016)
[5] D. Y. Huo, X. Yang, C. Han *et al.*, Chin. Phys. C **45**, 114104 (2021)
[6] D. Y. Huo, Z. Wei, K, Wu *et al.*, Phys. Rev. C **108**, 024608 (2023)
[7] K. -H. Schmidt, B. Jurado, C. Amouroux *et al.*, Nucl. Data Sheets **131**, 107 (2016)
[8] A. J. Koning, S. Hilaire, and S. Goriely, TALYS-1.8 User Manual (2015)
[9] D. M. Gorodisskiy, K. V. Kovalchuk, S. I. Mulgin *et al.*, J. Korean Phys. Society **59**, 919 (2011)
[10] S. A. Giuliani, Z. Matheson, W. Nazarewicz *et al.*, Rev. Mod. Phys. **91**(1), 011001 (2019)
[11] A. Bulgac, P. Magierski, K. J. Roche *et al.*, Phys. Rev. Lett. **116**(12), 122504 (2016)
[12] D. Regnier, N. Dubray, and N. Schunck, Phys. Rev. C **99**, 024611 (2019)
[13] Y. Aritomo, S. Chiba, and F. Ivanyuk, Phys. Rev. C **90**, 054609 (2014)
[14] A. J. Sierk, Phys. Rev. C **96**, 034603 (2017)
[15] J. Randrup and P. Möller, Phys. Rev. Lett. **106**, 132503 (2011)
[16] J. Randrup, P. Möller, and A. J. Sierk, Phys. Rev. C **84**, 034613 (2011)
[17] Y. Abe *et al.*, Phys. Rep. **275**, 49 (1996)
[18] J. Blocki *et al.*, Ann. Phys. (N. Y.) **113**, 330 (1978)
[19] C. L. Zhang, B. Schuetrumpf, and W. Nazarewicz, Phys. Rev. C **94**, 064323 (2016).
[20] C. Y. Wong, Phys. Rev. Lett. **31**, 766 (1973)
[21] H. Pasca, A. V. Andreev, G. G. Adamian *et al.*, Phys. Rev. C **93**, 054602 (2016)
[22] P. P. Dyachenko, B. D. Kuzminov, and M. Z. Tarasko, Sov. J. Nucl. Phys. **8**, 165 (1969)
[23] Y. G. Ma, K. Wang, J. G. Chen *et al.*, Phys. Rev. C **72**, 064603 (2005)
[24] J. Benlliure, A. Grewe, M. de Jong *et al.*, Nucl. Phys. A **628**, 458 (1998).
[25] F. -J. Hambsch and F. Vivès, Nucl. Phys. A **679**, 3 (1999)
[26] C. M. Zoeller, A. Gavron, J. P. Lestone *et al.*, Seminar on fission "Pont d'Oye III", Castle of Pontd'Oye, Habay-la-Neuve, Belgium (1995), p. 56
[27] N. I. Akimov and Vorob'eva, Y ad. Fiz. **13**, 484 (1971)
[28] I. V. Ryzhov, S. G. Yavshits, G. A. Tutin *et al.*, Phys. Rev. C **83**, 054603 (2011)